

# Transient ischemia/hypoxia enhances gentamicin ototoxicity via caspase-dependent cell death pathway

Chia-Der Lin<sup>1,2,\*</sup>, Ming-Ching Kao<sup>3,4</sup>, Ming-Hsui Tsai<sup>1,2</sup>, Chih-Ho Lai<sup>5,\*</sup>, I-Hua Wei<sup>6</sup>, Mang-Hung Tsai<sup>6</sup>, Chih-Hsin Tang<sup>7</sup>, Cheng-Wen Lin<sup>8</sup>, Chuan-Jen Hsu<sup>9</sup> and Ching-Yuang Lin<sup>2,10</sup>

Aminoglycoside ototoxicity is a common cause of drug-induced hearing loss. Toxicity is dose related, but some patients may still develop hearing loss even under safe dosage. Apart for genetic idiosyncrasy, indirect evidences imply that ischemia may increase the aminoglycoside ototoxic sensitivity because common clinical situations associated with cochlear ischemia such as noise, sepsis, and shock are known to augment the development of aminoglycoside ototoxicity. At present, a direct interaction of cochlear ischemia and aminoglycoside ototoxicity is still lacking. This study demonstrated a direct evidence of increased gentamicin (GM) ototoxic sensitivity in chronic guinea pig models of transient cochlear ischemia. No permanent auditory changes were observed after a single dose of GM (125 mg/kg) or after transient cochlear ischemia for 30 min. Persistent and significant auditory threshold shift was detected when GM was given after transient cochlear ischemia. Cochlear hair cells and spiral ganglion neurons are the major regions affected. Apoptosis contributes to hair cell death during acute interaction of ischemia and GM ototoxicity. Increased apoptotic cell death was also depicted when GM crossreacted with hypoxia *in vitro*, using cochlear cell lines. Generation of reactive oxygen species, loss of mitochondrial membrane potential, calcium release, and caspase-dependent apoptotic cell death were shown during the interaction of hypoxia and GM ototoxicity *in vitro*. This synergistic ototoxicity may be critical to aminoglycoside-induced hearing loss in clinical scenarios. The results should improve our understanding of the interacting mechanism and potential preventive strategy to aminoglycoside ototoxicity.

*Laboratory Investigation* (2011) 91, 1092–1106; doi:10.1038/labinvest.2011.69; published online 25 April 2011

**KEYWORDS:** aminoglycoside; guinea pig; hypoxia; *in vitro*; ischemia; ototoxicity

Aminoglycoside is an effective antibiotic against Gram-negative infection, widely used in clinical infections. Use of aminoglycoside has been shifted to less toxic antibiotics in industrialized countries because of its tissue-specific toxicity to the inner ear (ototoxicity) and kidney (nephrotoxicity). Still, in developing countries, aminoglycoside remains the frontline antibiotic because of its efficacy and low cost. Even the World Health Organization recommends it as an essential component of regimens to treat rising prevalence of multi-drug-resistant tuberculosis.<sup>1</sup> Aminoglycoside may be one of the most commonly used antibiotics worldwide.

The universal use of aminoglycoside makes its ototoxicity as a major cause in acquired hearing loss.<sup>2</sup> The pooled ototoxic rates of systemic aminoglycoside are ~2.0–2.3%.<sup>3</sup> although aminoglycoside ototoxicity correlates with cumulative dose and mode of drug administration, some patients develop cochlear dysfunction even under therapeutic dosage.<sup>4</sup> Supposedly safe dose of aminoglycoside does not always preclude ototoxicity. Besides dose-related toxic effects, susceptibility to aminoglycoside ototoxicity has been imputed to genetic idiosyncrasy, especially mitochondrial *12S rRNA* gene mutation<sup>5,6</sup> carried by an estimated 10–20% of

<sup>1</sup>Department of Otolaryngology-Head and Neck Surgery, China Medical University Hospital, Taichung, Taiwan; <sup>2</sup>Graduate Institute of Clinical Medical Science, School of Medicine, China Medical University, Taichung, Taiwan; <sup>3</sup>Department of Biological Science and Technology, College of Life Sciences, China Medical University, Taichung, Taiwan; <sup>4</sup>Department of Biochemistry, National Defense Medical Center, Taipei, Taiwan; <sup>5</sup>Department of Microbiology, School of Medicine, China Medical University, Taichung, Taiwan; <sup>6</sup>Department of Anatomy, School of Medicine, China Medical University, Taichung, Taiwan; <sup>7</sup>Department of Pharmacology, School of Medicine, China Medical University, Taichung, Taiwan; <sup>8</sup>Department of Medical Laboratory Science and Biotechnology, School of Medicine, China Medical University, Taichung, Taiwan; <sup>9</sup>Department of Otolaryngology-Head and Neck Surgery, National Taiwan University Hospital, Taipei, Taiwan and <sup>10</sup>Clinical Immunological Center, China Medical University Hospital, Taichung, Taiwan  
Correspondence: Professor C-Y Lin, MD, PhD, College of Medicine, China Medical University, Clinical Immunological Center, China Medical University Hospital, No. 2, Yuh-Der Road, Taichung, Taiwan 40402, Republic of China.  
E-mail: cylin@mail.cmuh.org.tw

\*These authors contributed equally to this work.

Received 26 August 2010; revised 11 February 2011; accepted 15 February 2011

such patients.<sup>7</sup> However, recent study shows that most patients with *12S rRNA* gene mutation do not exhibit evidence of hearing loss when exposed to aminoglycoside.<sup>8</sup> A more detailed investigation of the basic mechanism contributing to aminoglycoside ototoxicity is necessary.

Previous studies on predisposing factors for aminoglycoside ototoxicity point to drug–drug interaction,<sup>9,10</sup> underlying medical conditions,<sup>11</sup> and stress.<sup>12</sup> Comorbid conditions, such as perinatal asphyxia, hypovolemia, shock, or sepsis, were supposed to augment aminoglycoside ototoxicity.<sup>13–15</sup> Although multiple factors may confound these clinical situations, significant decrease of blood pressure is observed in hypovolemia, shock, or sepsis. Cochlear blood flow was observed to be stopped when acute reduction of blood pressure was induced in animals.<sup>16</sup> In humans, simply hypotension<sup>17</sup> or reduction in blood pressure in a previous hypertensive patient<sup>18</sup> may result in acute cochlear dysfunction manifested as sudden sensorineural hearing loss, supposedly caused by cochlear ischemia. It is plausible that cochlear hypoperfusion may be associated with the sensitivity of aminoglycoside ototoxicity. In addition, disturbance of cochlear microcirculation has been shown to be the fundamental mechanism contributing to common otologic disorders: for example, age-related<sup>19</sup> or noise-induced<sup>20,21</sup> hearing losses. Increased aminoglycoside ototoxicity was also shown in aging changes<sup>22</sup> and noise trauma.<sup>12,23</sup> These indirect evidences suggested that ischemia might be important in the development of aminoglycoside ototoxicity, but very few studies address the direct interaction of ischemia and aminoglycoside ototoxicity. This study investigated what aminoglycoside ototoxicity would go on after ischemia/reperfusion injury using a chronic guinea pig model of transient cochlear ischemia.<sup>24</sup> Then, we studied gentamicin (GM)-induced cell apoptosis in different hypoxic conditions using HEI-OC1 (House Ear Institute–Organ of Corti 1) cell lines. These results may help us understand the development of aminoglycoside ototoxicity when interacting with hypoxia/ischemia, for example, patients in critical condition or intensive care unit treated with aminoglycoside.

## MATERIALS AND METHODS

### Transient Cochlear Ischemia Model

Albino guinea pigs aged between 2 and 4 months (body weight 350–550 g) were used, with approval from the institutional animal care and use committee of China Medical University. Animals were anesthetized by intramuscular (i.m.) injection of a mixture of Zoletil (30 mg/kg; VIRBAC, Carros, France) and xylazine (10 mg/kg; Bayer, Leverkusen, Germany), allowing non-ventilator-dependent oxygenation. Maintenance dose, 50% of initial dose, was injected every 60 min thereafter. For surgical accessibility and convenience, only the left ear was used for this experiment and right cochlea was surgically destroyed to avoid acoustical crossover during auditory measurements. Ventral approach to labyrinthine artery has been described.<sup>24,25</sup> In brief, electrodes

were inserted subcutaneously into the left mastoid (anode), right mastoid (cathode), and back (ground) and an earphone inserted into the left ear canal to monitor auditory brainstem responses (ABRs) perioperatively. A submental incision was made medially to mandibular edge. The myofascial plane and digastric muscle were dissected to expose the tympanic bulla; a rongeur opened the thin bony shell of the tympanic bulla to expose basal cochlear turn. A fenestrum was drilled at the petrous bone, medially to the basal turn so that the labyrinthine artery was visible under the dura, which was excised to expose the labyrinthine artery, which in turn was closed with V1 microclamps (no. 00396-01; F.S.T., Foster City, CA, USA). Cochlear function was thereafter monitored by click ABRs at 120 decibel (dB) sound pressure level at least every 3 min. Compared with preoperative apparent ABR waveform, persistent absence of waveform indicated that microclamps had successfully occluded the labyrinthine artery.

The animals were divided into different groups ( $n = 6$  in each group). Control, no surgery; GM group, the animals received single dose of i.m. GM (125 mg/kg); sham operation (sham-op) group, the animals received the above surgical procedure until the labyrinthine artery was exposed temporarily without interruption; sham-op/GM group, the animals received single dose of i.m. GM (125 mg/kg) after sham-op; 30-min ischemia group, the animals received the above surgical procedure to induce transient cochlear ischemia for 30 min; 30-min ischemia/GM group, the animals received single dose of i.m. GM (125 mg/kg) after induction of transient cochlear ischemia for 30 min, described as above.

In each group, four cochleae were prepared for rhodamine-phalloidin staining and hair cell (HC) counting. The cochleae of the other two animals were stained with hematoxylin/eosin after paramodiolar section.

### Auditory Test

Auditory test was performed by tone burst ABRs in a sound-attenuated room. The pure tone bursts were generated with the amplitude specified by a real-time programmable attenuator (Intelligent Hearing Systems, IHS Smart EP version 3.97, Miami, FL, USA) with ER2 insert earphone, with stimulus frequency at 1, 2, 4, 8, and 16 kHz (0.2 ms rise/fall time and 1 ms flat segment) with maximal output level 125, 123, 111, 117, and 98 dB sound pressure level. The click/tone bursts were produced by IHS high-frequency transducer in a closed acoustic system through the sound delivery system. Responses for 1024 sweeps were averaged at each intensity level around the threshold in 5 dB steps. Threshold was defined as the lowest intensity at which a clear waveform was visible upon inspection of an evoked trace. Each ABR threshold was compared with the preoperative threshold, which served as the baseline measurement. Serial ABR measurements were performed preoperatively, immediately after the operation, at 3 days after the operation, and 1, 2, and 4 weeks after the operation.

### Cochlea HC Counting after Rhodamine-Phalloidin Staining

Following the study, animals were deeply anesthetized and decapitated. The left cochleae were fixed with 4% paraformaldehyde in 0.1 M phosphate-buffered saline (PBS) by perilymphatic perfusion and immersed in the same fixative for 1 day. The organ of Corti was dissected. Tissues were permeabilized with 0.3% Triton X-100 for 10 min and incubated with rhodamine-coupled phalloidin (Molecular Probes, Eugene, OR, USA) for 30 min. Strips of the organ of Corti were divided into four turns, mounted on glass slides, and examined by fluorescent microscope to count the number of HCs present at each cochlear turn, thereby determining the extent of HC loss.

### Histopathological Examination

Cochlear sectioning along the paramodiolar axis was followed by hematoxylin/eosin staining. After fixation as described above, cochleae were decalcified in 10% ethylenediamine tetra-acetic acid for 4 weeks at 4 °C, then dehydrated, embedded in paraffin, and sectioned serially (4 μm thick) parallel to the modiolar axis. Sections were plated for hematoxylin/eosin staining and examined under a high-power light microscope.

### Tracking GM Uptake Using Fluorescence GM

The fluorescence-conjugated GM made by conjugation of Texas Red (TR) esters and GM was used to track the distribution of GM in the cochlea, according to previous studies.<sup>26,27</sup> In brief, 2.2 ml of GM sulfate (Sigma, St Louis, MO, USA; 50 mg/ml in 100 mM K<sub>2</sub>CO<sub>3</sub> at pH 9.0) and 0.6 ml of succinimidyl esters of TR (Molecular Probes; 2 mg/ml in dimethyl formamide) were mixed and agitated at 4 °C overnight to produce a GM–Texas Red conjugate (GMTR). A high molar ratio (~150:1) of GM to TR was used to prevent overlabeling GM molecule with more than one TR molecule and ensure the polycationic nature of conjugated GMTR.<sup>27</sup> The left ear of the animal underwent transient cochlear ischemia of 30 min as described above and the right ear served as control. Immediately after the surgery, GM/GMTR (125 or 250 mg/kg) was injected subcutaneously. The animals were killed 30, 90, or 180 min later. The cochleae were harvested and fixed with 4% paraformaldehyde in 0.1 M PBS by perilymphatic perfusion and immersed in the same fixative for 1 day. The organ of Corti was dissected, mounted on glass slides, and examined by fluorescence microscopy. For image analysis, the images of the cochlear strips from the middle cochlear turn in each experimental group were identified and regions of interest (inner hair cells (IHCs) and rows of outer hair cells (OHCs)) were manually segmented for pixel fluorescence intensity determination using the image analyzer (Image Pro Plus VI, Media Cybernetics, Silver Spring, MD, USA). The relative mean fluorescence intensity was ratioed against the reference (the intensity of first row of

OHCs 30 min after 125 mg/kg GM/GMTR injection in the control cochlea) and plotted.

### *In Situ* Detection of Nuclear DNA Fragmentation *In Vivo*

We used the terminal deoxynucleotidyl transferase (TdT)-mediated deoxyuridine triphosphate (dUTP)-biotin nick end labeling (TUNEL) method to detect DNA fragmentation after the combination of GM and cochlear ischemia. The animals, which received a single dose of GM (125 mg/kg) after induction of transient cochlear ischemia for 30 min, were killed 1, 3, and 7 days after the operation ( $n = 2$ , in each time point). The organ of Corti was dissected after fixation processes. The specimens were stained with a modified TUNEL method using an *in situ* cell death kit-fluorescein (Roche Diagnostics, Mannheim, Germany). The tissues were pretreated with permeabilization solution (0.1% Triton X-100 in 0.1% sodium citrate) on ice for 2 min, and then incubated for 60 min at 37 °C with the TUNEL reaction mixture. After washing in PBS, sections were photographed in a laser scanning confocal microscope (Zeiss LSM510, Carl Zeiss, Göttingen, Germany).

### *In Vitro* Cell Culture System and Induction of Hypoxia

The HEI-OC1 cells were cultured in DMEM (Invitrogen, Carlsbad, CA, USA) supplemented with 10% FBS (HyClone, Logan, UT, USA) and maintained at 33 °C under 5% CO<sub>2</sub> in air. For the generation of hypoxic condition, cells were cultured in 95% N<sub>2</sub> and 5% CO<sub>2</sub> (Anaerobic System PROOX model 110; BioSpherix) condition and incubated at 33 °C within the chamber for 24 h. Cells incubated in hypoxia condition for 0–24 h did not affect cell viability by cell viability assay (data not shown).

### Analysis of Cell Viability

After treatment with GM under hypoxic condition for the indicated time intervals, cultured cells were washed with PBS. The 3-(4,5-dimethylthiazol-2-yl)-2,5-diphenyl tetrazolium bromide (MTT) assay was used to test the cytotoxicity of GM in cells as described previously.<sup>28</sup>

### Quantification of Apoptosis by Flow Cytometry

Cells were treated with vehicle or GM and cultured in hypoxia for the indicated time intervals. After treatment, cells were washed twice with PBS, and resuspended in staining buffer containing 1 μg/ml PI and 0.025 μg/ml Annexin V-FITC. Cells were analyzed using FACScan and the Cellquest program (Becton Dickinson, Lincoln Park, NJ, USA).

Further quantitative assessment of apoptotic cells was detected using TUNEL assay (Roche Diagnostics) according to the manufacturer's instructions. The stained cells were then analyzed using a FACScan and the Cellquest program (Becton Dickinson).

### Determination of the Mitochondrial Membrane Potential

The mitochondrial membrane potential ( $\Delta\psi_m$ ) was assessed using a fluorometric probe JC-1 (Calbiochem, San Diego, CA, USA), with a positive charge of a mitochondrial-specific fluorophore, indicated by a fluorescence emission shift from green (525 nm) to red (610 nm). Cells were plated in six-well culture dishes and treated with vehicle or GM. After incubation, cells were stained with JC-1 (5  $\mu\text{g}/\text{ml}$ ) for 15 min at 37 °C. Samples were analyzed by FACScan using an argon laser (488 nm). Mitochondrial depolarization is specifically indicated by a decrease in the red to green fluorescence intensity ratio and analyzed by a FACScan and the Cellquest program (Becton Dickinson).

### Measurements of Reactive Oxygen Species (ROS)

To detect the level of ROS production, cells were loaded with 10  $\mu\text{M}$  dihydrorhodamine 123 (DHR 123) for 15 min. The fluorescence intensities were obtained by recording the FITC fluorescence. Cells were collected and analyzed by a FACScan and the Cellquest program (Becton Dickinson).

### Detection of $\text{Ca}^{2+}$ Concentrations

HEI-OC1 cells ( $5 \times 10^5$  cells/well) were cultured in 12-well plates with GM in hypoxia for the indicated time intervals to detect changes in  $\text{Ca}^{2+}$  levels. Cells were harvested and washed twice, resuspended in FURA-PE3/AM (3  $\mu\text{M}$ ) at 37 °C for 30 min, and analyzed by a FACScan and the Cellquest program (Becton Dickinson).

### Western Blot Analysis

Proteins of the cellular lysates were resolved on SDS-PAGE and transferred to Immobilon polyvinylidene difluoride membranes (Millipore, Billerica, MA, USA). The blots were blocked with 5% skim milk for 1 h at room temperature and then probed with antibodies against Bcl-2, Bcl-xl, Bax, Bak, caspase 3, caspase 9, PARP, calpain-1, and calpain-2 (Cell Signaling, Danvers, MA, USA; 1:1000) for 1 h at room temperature. After three washes, the blots were subsequently incubated with a donkey anti-rabbit peroxidase-conjugated secondary antibody (Santa Cruz Biotechnology, Santa Cruz, CA, USA; 1:1000) for 1 h at room temperature. The blots were visualized by enhanced chemiluminescence using Kodak X-OMAT LS film (Eastman Kodak, Rochester, NY, USA).

### Determination of Caspase Activity

The assay is based on the ability of the active enzyme to cleave the chromophore from the enzyme substrate LEHD-pNA (for caspase 9) and Ac-DEVD-pNA (for caspase 3; Promega, Madison, WI, USA). The cell lysates were prepared and incubated with specific anti-caspase 9 and caspase 3 antibodies. Immunocomplexes were incubated with peptide substrate in assay buffer (100 mM NaCl, 50 mM

4-(2-hydroxyethyl)-1-piperazine-ethanesulphonic acid, 10 mM dithiothreitol, 1 mM EDTA, 10% glycerol, 0.1% 3-[(3-cholamidopropyl)dimethylammonio]-1-propanesulfonate, pH 7.4) for 2 h at 37 °C. The release of *p*-nitroaniline was monitored at 405 nm. Results are represented as the percent change of the activity compared with the untreated control.

### Statistics Analysis

The ABR threshold shifts, the fluorescence intensities after fluorescence GM injection between control and ischemic cochlea, and the percentages of HC loss between the control and the sham-op group, and between the control and each of the treatment groups, were analyzed using the nonparametric Mann-Whitney *U*-test. The *in vitro* statistical analysis between two samples was performed using Student's *t*-test. *In vitro* statistical comparisons of more than two groups were performed using one-way analysis of variance (ANOVA) test. The statistical software was the SPSS program (version 12.0 for Windows, SPSS, Chicago, IL, USA). In all cases,  $P < 0.05$  was considered as significant.

## RESULTS

### Transient Ischemia Increases the GM-Induced Auditory Threshold Shifts

No significant auditory threshold changes were noted in the control, GM, sham-op, and sham-op/GM groups from 1 k to 16 kHz (Figure 1). The ABR thresholds increased immediately after 30-min ischemia, but such ABR threshold elevation soon returned to nearly baseline level in 3 days (Figure 1). When a single dose of GM at 125 mg/kg was given immediately after 30-min ischemia, persistent ABR threshold elevations were shown without significant recovery (Figure 1). After 4 weeks, the ABR threshold elevations for the GM, sham-op, sham-op/GM, and 30-min ischemia groups were not significantly different from the control group at all frequencies tested. The ABR threshold shifts at 4 weeks after a combination of GM and 30-min ischemia were  $\sim 60$  dB (1 kHz:  $44.2 \pm 5.3$ , 2 kHz:  $46.7 \pm 6.6$ , 4 kHz:  $67.5 \pm 5.0$ , 8 kHz:  $68.3 \pm 6.8$ , 16 kHz:  $70.8 \pm 5.1$ , in dB, mean  $\pm$  s.e.), significantly different from the control group. The ABR threshold shifts 4 weeks after a combination of 30-min ischemia and GM showed more severe threshold shifts in higher frequencies (4–16 kHz) than at lower frequencies (1–2 kHz).

### Increased HC Loss After Interaction of GM and Ischemia

Most IHCs were preserved in all experimental groups, except for the basal ( $42.1 \pm 20.8\%$  loss) and second ( $42.8 \pm 16.2\%$  loss) turns in the 30-min ischemia/GM group, significantly different from the other groups. Remarkable OHC loss was observed in the 30-min ischemia/GM group, mainly in the basal and second turns, where  $>80\%$  loss was observed (Figure 2a). Fairly normal morphology of IHCs in the third

and apical turns was present. Variable degrees of OHC loss were found in the upper turns of the 30-min ischemia/GM group (Figure 2c). No significant differences appeared in HC loss in control, GM, sham-op, sham-op/GM, and 30-min ischemia groups.

**Organ of Corti and Spiral Ganglion Neurons Were Mostly Affected 4 Weeks After Co-Administration of GM and Transient Cochlear Ischemia**

No significant morphological changes were observed in the groups without significant changes in hearing level, such as

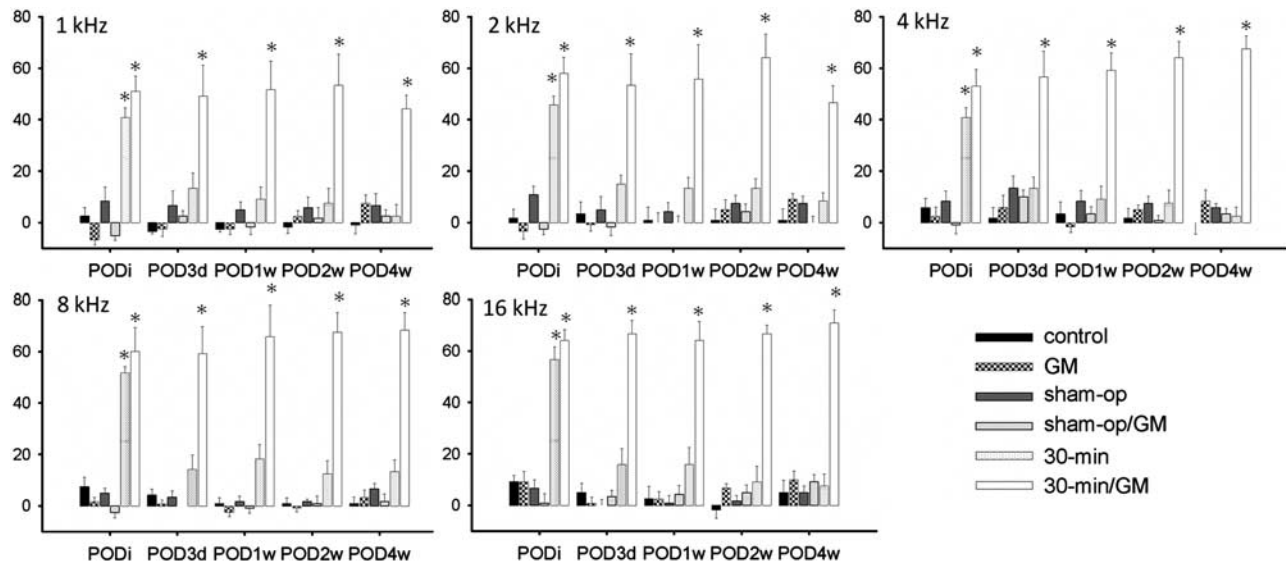


**Figure 1** Serial auditory threshold shifts in different groups (control, black; gentamicin alone (GM), checker; sham-op, deep gray; sham-op + gentamicin (sham-op/GM), gray; 30-min ischemia, dotted; 30-min ischemia then gentamicin (30-min/GM), white;  $n = 6$  in each group) after different durations of follow-up. The ABR was recorded by different tone burst stimulation from 1 to 16 kHz. Transient auditory shifts were depicted in the 30-min ischemia group whereas persistent auditory threshold elevations were shown in the 30-min/gentamicin group. No significant auditory changes were noted in the other groups. The y axis indicates the auditory threshold shifts in decibel (dB). The x axis indicates the timing for serial auditory measurement, from baseline, immediately (PODi), and at 3 days, and 1, 2, and 4 weeks after operation (POD3d, 1w, 2w, 3w, and 4w). POD: postoperation day. The value with error bar in each point indicates mean  $\pm$  s.e. The value in each group was compared with that in the control ( $*P < 0.001$ ).

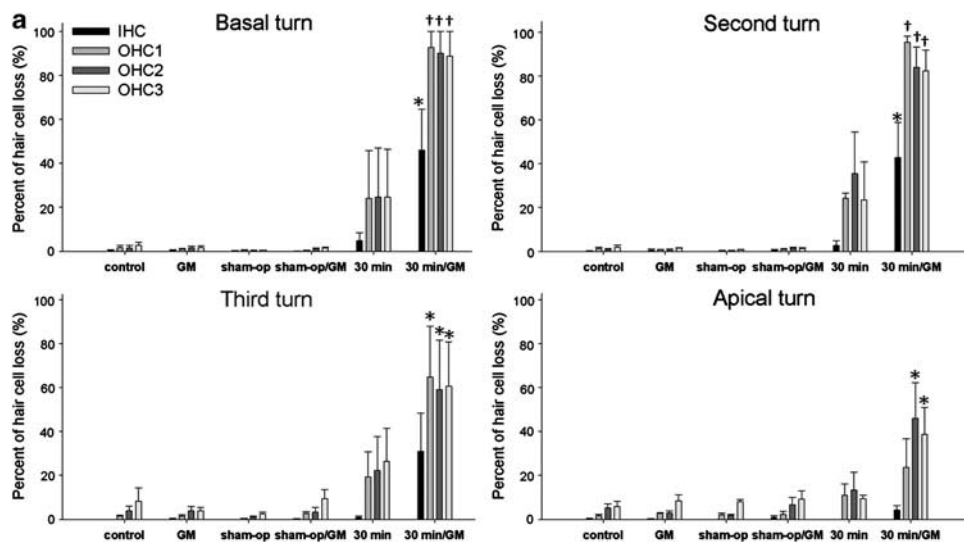


**Figure 2 (a)** Hair cell losses (inner hair cell (IHC); first, second, and third row of outer hair cell (OHC1, 2, 3)) in different groups ( $n = 4$  in each group) at different cochlear turns. Compared with the control group, significant hair cell loss was depicted when the administration of gentamicin was given after transient cochlear ischemia, especially in the basal turn. The y axis indicates percents of hair cell loss. The x axis indicates different treatment groups, from control, GM, sham-op, sham-op/GM, 30-min ischemia, and 30-min ischemia/GM. The value with error bar in each point indicates mean  $\pm$  s.e. ( $*P < 0.05$ ;  $†P < 0.001$ ).

**(b)** Rhodamine-phalloidin staining of actin after surface preparation of cochlea in the sham-op/GM group showed the normal and well-defined outline of three rows of OHCs and one row of IHCs. **(c)** Representative morphology of hair cell labeling with rhodamine-conjugated phalloidin in animals treated with gentamicin after 30-min ischemia. Complete loss of IHCs and the three rows of OHCs were depicted in the basal turn. Partial loss of IHCs and complete loss of OHCs could be identified in the second turn. Asterisks indicate individual IHC loss in the second turn and OHC loss in the third and apical turns. Bar = 20  $\mu$ m.

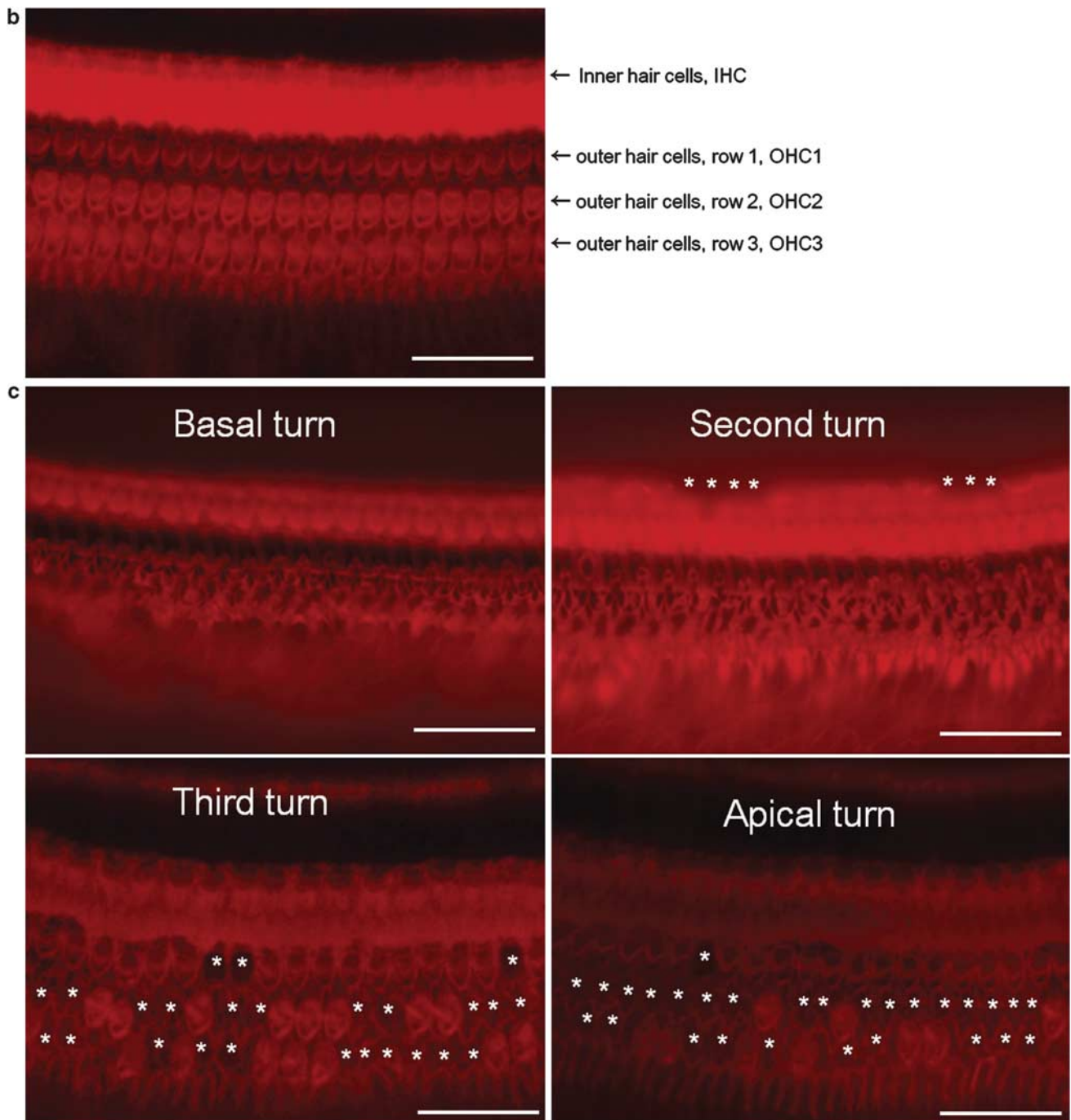


**Figure 2** Continued.

the control, GM, sham-op, sham-op/GM, or 30-min ischemia group (not depicted). In the animals that received GM after 30-min ischemia, obvious morphologic changes were observed in basal cochlear turns and minimal changes in upper cochlear turns. Distortion of organ of Corti with collapsed Corti's tunnel was seen with loss of spiral ganglion neurons in basal cochlear turns from 30-min ischemia/GM animals (Figure 3e and f). However, morphology of stria vascularis seemed not to change much in lower and upper

turns (Figure 3a and d). In upper turns, organs of Corti retained their architecture, with distribution of spiral ganglion neurons fairly normal (Figure 3b and c).

#### **Enhanced GM Uptake After Transient Cochlear Ischemia**

For the animals receiving 125 mg/kg GM/GTTR injection, faint GMTR fluorescence was depicted in the OHCs 30 min after the application of GM/GTTR (Figure 4a and d). The IHCs displayed GMTR fluorescence 90 min later in the

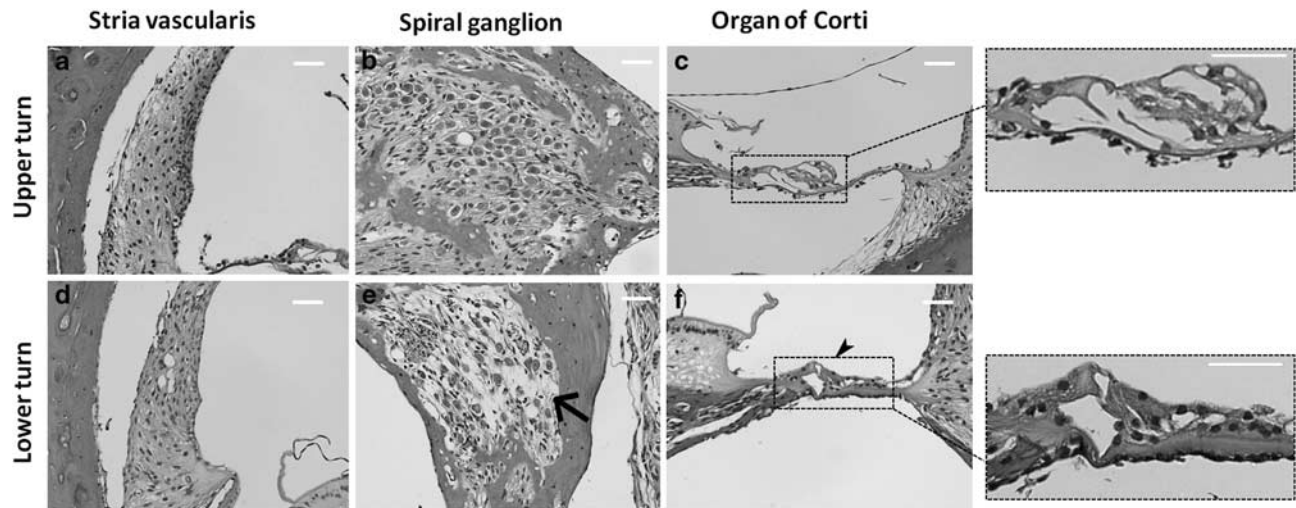


**Figure 3** Representative sections in upper turn (a–c) and lower turn (d–f) of the cochlea from the animals that received gentamicin after 30-min ischemia. The histopathology of the stria vascularis (a, d), spiral ganglion (b, e), and organ of Corti (c, f) was depicted. Partial loss of spiral ganglion cells (arrow) and dysmorphic arrangement in the organ of Corti (arrowhead) was noted in the lower turns of cochlea, compared with those in the upper turns. Higher magnifications of Organ of Corti were illustrated in the right block diagrams. Bar = 20  $\mu$ m.

30-min ischemic cochlea (Figure 4e), but were negligibly visible in the control cochlea (Figure 4b). The GMTR fluorescence was also found in the cytoplasm of sporadic OHCs 90 min after GM/GMTR injection, which was more prominent in the 30-min ischemic cochlea (Figure 4b and e). Apparent cytoplasmic GMTR fluorescence labeling in HCs was visible 180 min later, in which it was more intensely labeled in the 30-min ischemic cochlea (Figure 4c and f). The GMTR fluorescence was brighter in the ischemic cochlea than that in the control ones, especially 180 min after GMTR injection (Figure 4g).

More distinct GMTR fluorescence was depicted in the cochlea with higher dosage of GM/GMTR (250 mg/kg) than in those with lower dosage (125 mg/kg) (Supplementary Figure 1). Similarly, the ischemic cochlea displayed more GMTR fluorescence than the control cochlea.

#### Apoptosis Contributes to the HC Death in the Acute Interaction of GM and Transient Cochlear Ischemia *In Vivo*

TUNEL assay was used to detect DNA fragmentation after a combination of GM and cochlear ischemia. Representative TUNEL staining of HCs in the basal turns at 1, 3, and 7 days after co-administration of GM immediately after 30-min ischemia is shown in Figure 5. OHCs were observed to be labeled with TUNEL fluorescence 1 day after co-treatment, and IHCs after 3 days. TUNEL-stained positive cells were not observed 7 days later. Positive control procedure for the TUNEL method labeled all nuclei, and the negative control procedure labeled no nuclei in specimens.

#### Increased GM-Induced Cell Apoptosis During Hypoxia in HEI-OC1 Cells

To investigate the potential cell death form of GM in cochlear cells under a hypoxia environment (0.5%  $O_2$ ), we first evaluated the cell viability of HEI-OC1 cells under both hypoxia and normal oxygen conditions. As shown in Figure 6a, HEI-OC1 cells were treated with GM (0–40  $\mu$ M) for 24 h, and the cell viability was only slightly reduced, as analyzed by MTT assay. However, treatment of HEI-OC1 cells with GM under hypoxia conditions induced cell death in a concentration-dependent manner. Significant decrease of cell viability was observed ranging from 4 to 40  $\mu$ M (Figure 6a). Cells were then treated with 20  $\mu$ M GM under hypoxia conditions, revealing dramatically decreased cell viability in a time-dependent manner when compared with cells under normal oxygen conditions (Figure 6b). Therefore, our results suggested that hypoxia and GM treatment have a synergistic effect on ototoxicity based on *in vitro* study. We next investigated whether GM induces cell death through an apoptotic mechanism. Compared with vehicle-treated HEI-OC1 cells, high proportion of Annexin V<sup>+</sup> labeling was detected in HEI-OC1 cells treated with GM in hypoxia (Figure 7a). In addition, GM induced apoptosis in HEI-OC1 cells in a concentration-dependent manner (Figure 7b–e). Compared with vehicle-treated cells, those treated with GM showed significant cell apoptosis by TUNEL assay (Supplementary Figure 2).

#### More Mitochondrial Dysfunction Developed After GM Interacting with Hypoxia in HEI-OC1 Cells

Figure 8a shows that treatment of cells with GM at 20  $\mu$ M concentration for 0–24 h induced the loss of mitochondrial



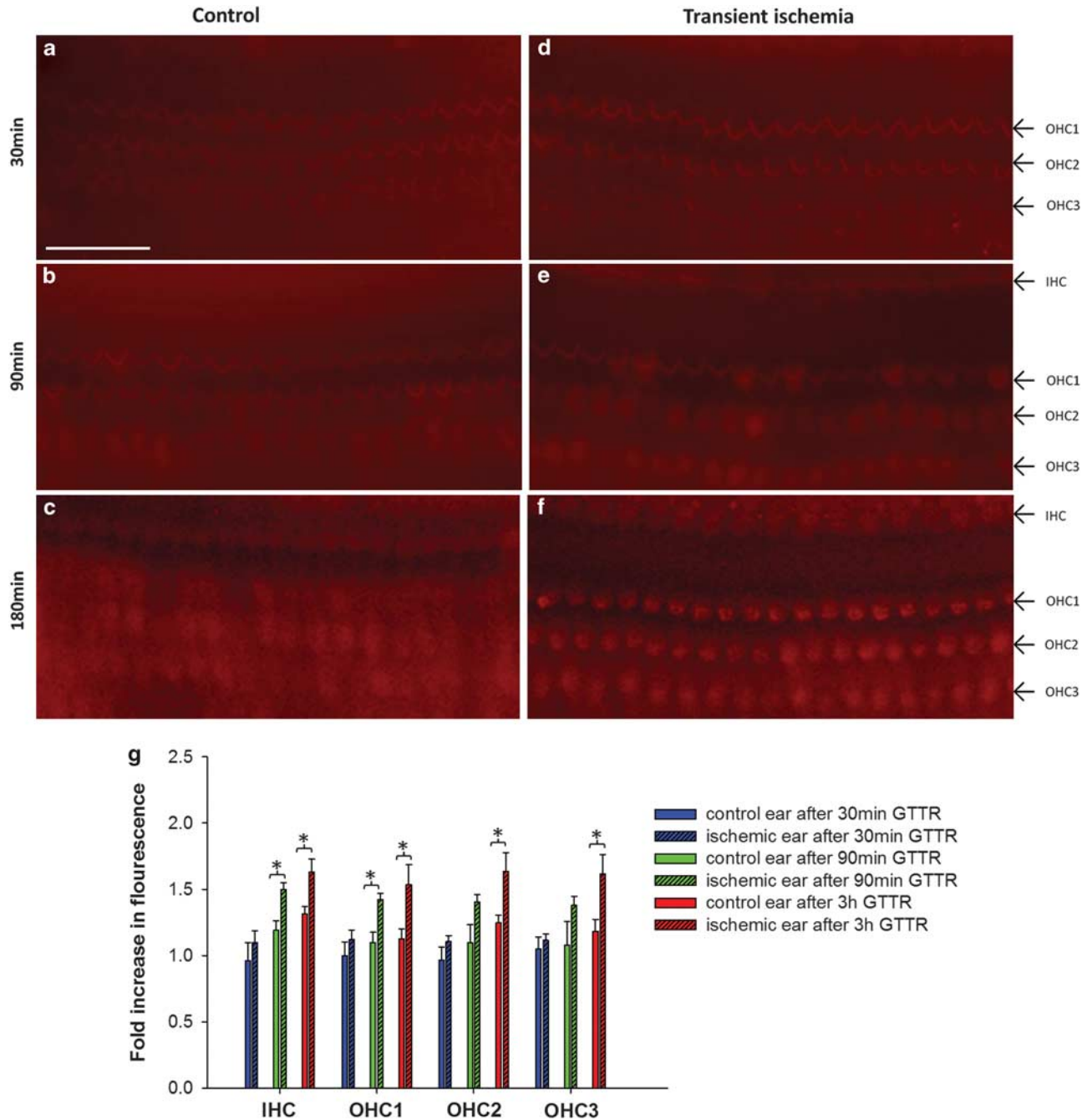


**Figure 4** Sequential GMTR fluorescence in the middle cochlear turn examined at 30, 90, and 180 min after 125 mg/kg GM/GMTR injection in the control (a–c) and 30-min ischemic cochlea (d–f). GMTR fluorescence in outer hair cells was depicted 30 min after injection of GMTR in both groups (a, d). At 90 min after application of GMTR, gentamicin fluorescence was still negligibly labeled at the inner hair cell of the control (b) but visible in those of the 30-min ischemic cochlea. Diffusion of GMTR fluorescence into hair cell cytoplasm could be found, especially in the ischemic cochlea (e). After 180 min, diffused GMTR fluorescence was labeled in the outer hair cells cytoplasm and some soma of inner hair cells (c, f), in which more intense GMTR fluorescence was labeled in 30-min ischemic cochlea (f). (g) Comparison of the sequential hair cells fluorescence differences between control and ischemic cochlea ( $n = 4$  in each group). The GMTR fluorescence is more intense in the outer hair cells. In addition, the hair cells in the ischemic cochlea exhibit more fluorescent intensity than those in the control cochlea at least 90 min after GMTR injection. The y axis indicates the relative fluorescence intensity ratioed against that of the first row of OHCs 30 min after 125 mg/kg GM/GMTR injection in the control cochlea. The x axis indicates the different hair cell types. The value with error bar in each point indicates mean  $\pm$  s.e. ( $*P < 0.05$ ) GM: gentamicin; GMTR: conjugate of gentamicin and Texas-Red esters. Bar = 20  $\mu$ m.

membrane potential in a time-dependent manner. We further examined whether accumulation of ROS was involved in GM-induced cell death. DHR-based flow cytometry analysis

revealed that intracellular  $O_2^-$  level increased in HEI-OC1 cells following treatment with GM under hypoxia condition (Figure 8b). To ascertain GM-induced HEI-OC1 cell



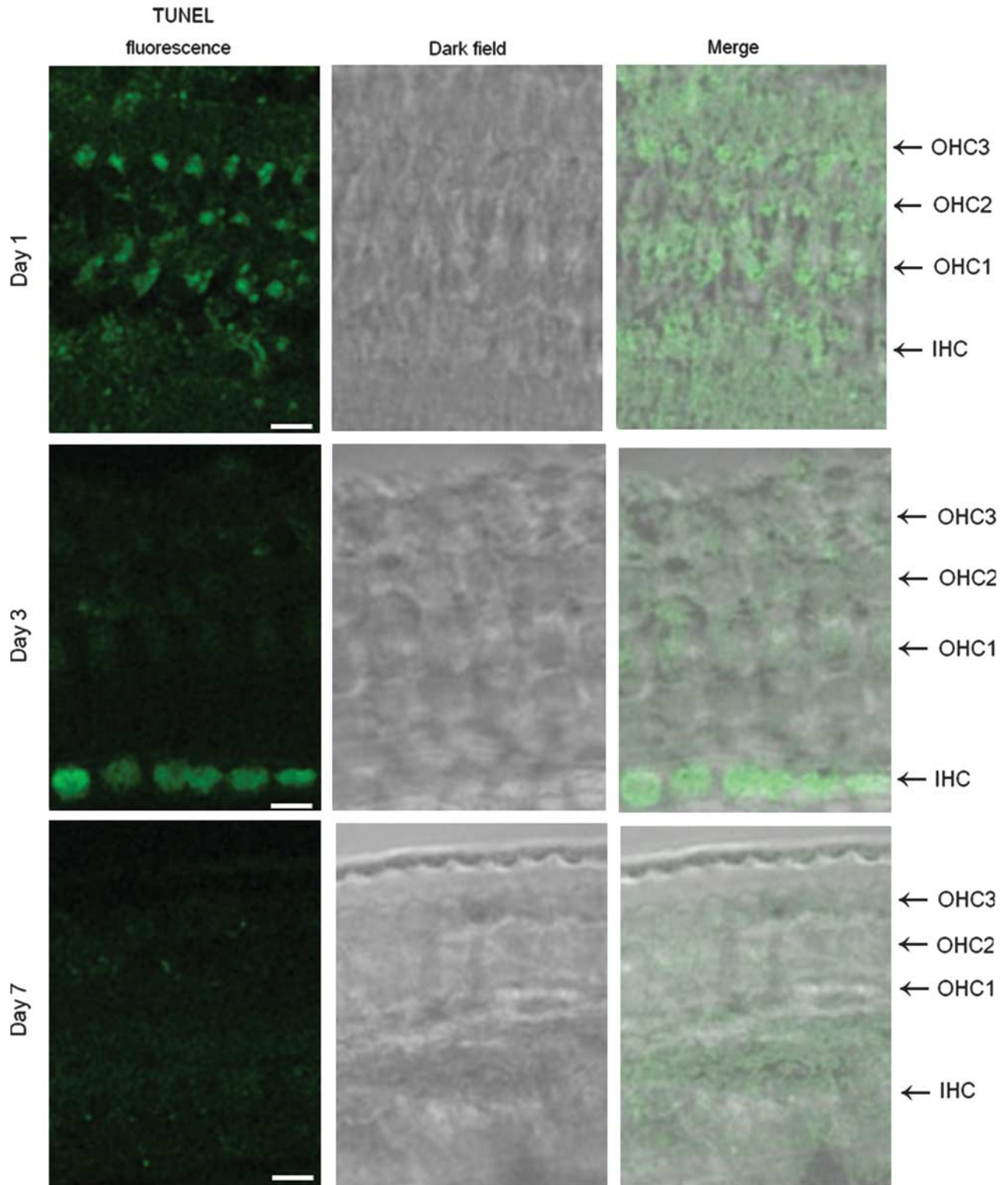


**Figure 5** Hair cells staining with TUNEL fluorescence seen at 1, 3, and 7 days in animals treated with gentamicin after 30-min ischemia. OHC labeling by TUNEL fluorescence was observed 1 day after combination of gentamicin and 30-min ischemia. After 3 days, IHC labeling with TUNEL fluorescence was observed. Bar = 10  $\mu$ m.

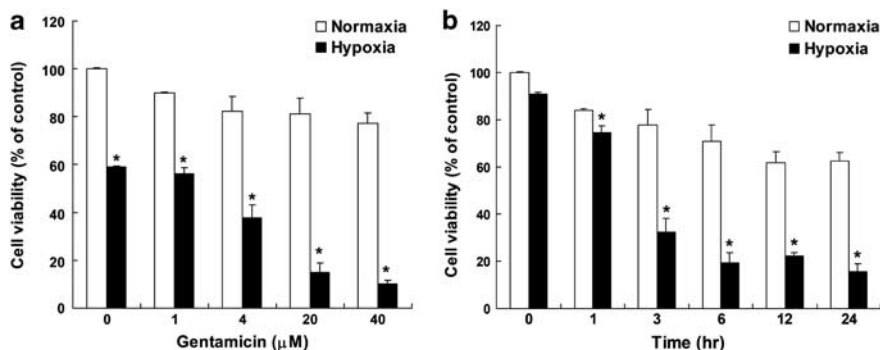


**Figure 6** Gentamicin-induced cell death of cultured cochlear cells. (a) HEI-OC1 cells were incubated with various concentrations of gentamicin for 24 h under normal oxygen and hypoxia conditions, and cell viability was examined by MTT assay ( $n=6$ ). (b) HEI-OC1 cells were incubated with gentamicin (20  $\mu\text{M}$ ) for different time intervals under normal oxygen or hypoxia conditions, and the cell viability was examined by MTT assay ( $n=6$ ). Open bar, normal oxygen condition; closed bar, hypoxia condition. Results are represented as the mean  $\pm$  s.d. \* $P<0.05$  when compared with control group.

apoptosis by triggering the mitochondrial apoptotic pathway, we measured change in expression of Bcl-2 family proteins. Quantitative densitometry showed that treatment of HEI-OC1 cells with GM under hypoxia condition induced an increase in Bax and Bak protein levels (Figure 8c). In addition, GM reduced expression of Bcl-2, which led to an increase in the proapoptotic/antiapoptotic Bcl-2 ratio (Figure 8c). These data suggest that mitochondrial dysfunction is involved in the cell apoptosis caused by interaction of hypoxia and GM in HEI-OC1 cells.

#### GM/Hypoxia Interaction Induces More Endoplasmic Reticulum (ER) Stress, $\text{Ca}^{2+}$ Release, and Calpain Activity

We further assessed the effect of GM on mobilization of  $\text{Ca}^{2+}$  in HEI-OC1 cells. When cells were cultured in hypoxia and treated with GM,  $\text{Ca}^{2+}$  levels significantly increased compared with the vehicle-treated control (Figure 9a). The data also demonstrated that GM promoted a  $\text{Ca}^{2+}$  flux in a time-dependent manner (Figure 9a). We further tested whether activity of calpain would be induced by GM in HEI-OC1 cells under hypoxia condition. The protein expression of calpain-1 and calpain-2 upon treatment of cell with GM under hypoxia conditions was analyzed. Quantitative densitometry showed that GM increased calpain-1 and calpain-2 expression in a time-dependent manner (Figure 9b), indicating  $\text{Ca}^{2+}$  release and calpain activity involved in cell death during interaction of GM and hypoxia in HEI-OC1 cells. We next examined the effects of GM on expression of caspase-9 and caspase-3 in HEI-OC1 cells. Our data showed that GM increased activation of both caspase-9 and caspase-3 in a concentration-dependent manner in HEI-OC1 cells, using western blot analysis (Figure 9c) as well as ELISA assay (Figure 9d). Nevertheless, the expressions of caspase-9 and caspase-3 were decreased upon treated with high concentration of GM at 20  $\mu\text{M}$  because of the cell death at this concentration. Additionally, treatment of cells with caspase-3 and caspase-9 inhibitors reduced GM-induced apoptosis of cells (Figure 9e), indicating GM-induced cell apoptosis

during hypoxia status as mediated via mitochondrial dysfunction, ER stress, and caspase cascade.

#### DISCUSSION

This study showed transient hearing loss without obvious HC loss at 4 weeks after transient cochlear ischemia of 30 min (Figures 1 and 2), reflecting a revival potential of cochlea to transient ischemia in guinea pigs may be up to 30 min.<sup>24,25</sup> The administration of GM in 125 mg/kg alone could not produce prolonged significant ABR threshold shifts or HC loss, consistent with previous study.<sup>29</sup> However, administration of GM after transient cochlear ischemia elicited significant auditory threshold shifts (Figure 1). The hearing deterioration was considered permanent, because no recovery in auditory threshold was observed by 4 weeks after treatment, and there was significant loss of cochlear HCs, which cannot be regenerated in mammals.

Our results also showed that auditory threshold shifts correlated more with the high frequency (4–16 kHz) than with low frequency (1–2 kHz; Figure 1). These observations were confirmed by morphological examination of cochlear surface preparation and numbers of HCs stained with phalloidin (Figure 2). The basal-turn HCs, which represent higher frequency, seemed more susceptible to damage than upper-turn HCs, which represent lower frequency (Figure 2). HCs are the primary targets during aminoglycoside ototoxicity. Flattening of Corti's tunnel was observed 6 months after administration of toxic dose of aminoglycoside.<sup>30</sup> In this study, dysmorphic organ of Corti in the basal turn was observed 4 weeks after the interaction of GM and ischemia (Figure 3f). This may signify that ischemia may exacerbate and fasten the GM ototoxicity.

Ototoxicity of aminoglycosides to cochlear HCs also progresses in a base-to-apex gradient.<sup>2</sup> The uptake of GM by HCs in the basal turns is greater than that in apical turns.<sup>31</sup> The basal portion of the cochlea has a greater rate of oxygen consumption than does the upper apical portion.<sup>32</sup> Conversely, the energy reserve of the organ of Corti, especially glycogen, follows an inverse base-to-apex distribution—more

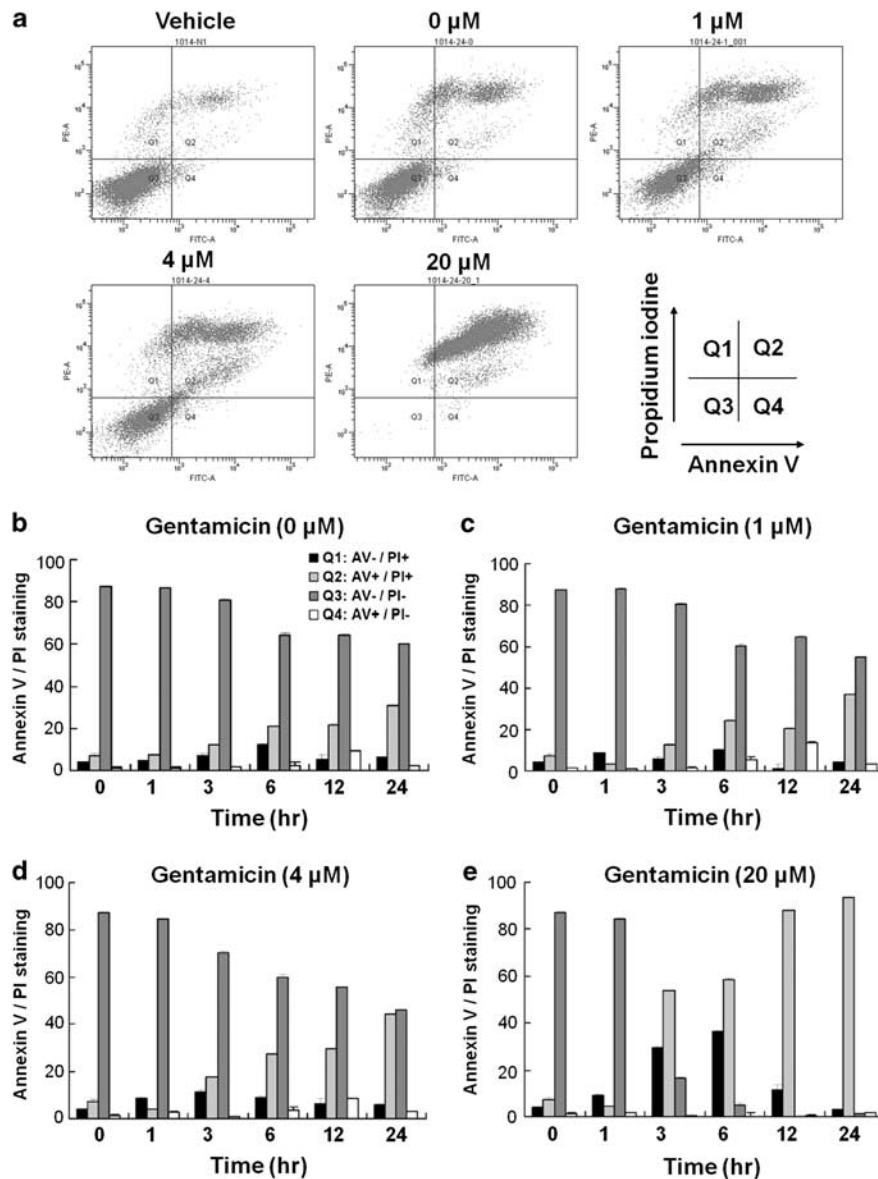


**Figure 7** Gentamicin-induced apoptosis of cultured cochlear cells. (a) HEI-OC1 cells were treated with vehicle or various concentrations of gentamicin for 24 h under hypoxia condition, and the percentage of apoptotic cells was assessed by flow cytometric analysis of Annexin V/PI staining ( $n = 3$ ). (b–e) Relative levels of apoptotic cells were calculated. Results are expressed as the mean  $\pm$  s.d.

glycogen is found in apical turns than in basal turns.<sup>33</sup> A base-to-apex gradient of differential intrinsic susceptibility to free radicals has also been noted.<sup>34</sup> The HCs in basal turns are more vulnerable to free-radical damage than those in apical turns,<sup>34</sup> which could explain why apical turns better tolerate damage from co-administered GM/ischemia.

Besides intrinsic base-to-apical differential susceptibility to ischemia, this study showed guinea pig OHCs more vulnerable to combined GM/ischemia than IHCs. OHCs have also proven more vulnerable to GM ototoxicity than IHCs.<sup>35–37</sup> It is still unclear why IHCs could tolerate aminoglycoside ototoxicity better than OHCs. Similar results were observed

in mice, as observation of OHC loss by GM ototoxicity precedes IHC loss.<sup>2</sup> After 4 weeks, minimal OHC loss occurred when ischemia lasted 30 min, but significant OHC loss in nearly every cochlear turn was apparent after combined GM/ischemia treatment (Figure 2). The OHCs of guinea pigs might prove more vulnerable to ischemia/reperfusion injury than IHCs.<sup>24,38</sup> Besides ischemic damage, OHCs in guinea pigs are more vulnerable to other cochlear injuries, such as aminoglycoside ototoxicity.<sup>39</sup> Longer periods of ischemia may affect both IHCs and OHCs.

We also found spiral ganglion neurons damaged 4 weeks after combined GM/ischemia treatment, especially in lower (basal and second) cochlear turns where HCs were mostly

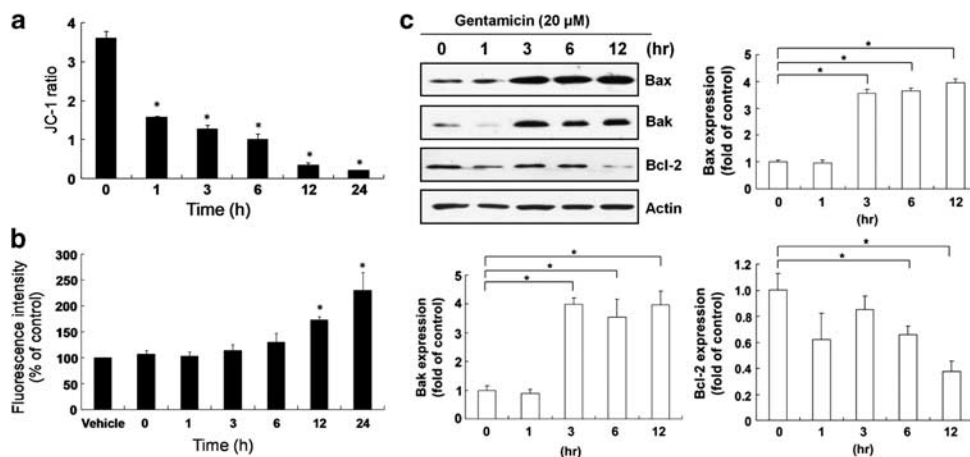


**Figure 8** Gentamicin induced mitochondrial dysfunction in cultured cochlear cells. HEI-OC1 cells were treated with gentamicin (20  $\mu$ M) for different time intervals under hypoxia condition, and (a) mitochondrial membrane potential and (b) the level of ROS production were examined by flow cytometric analysis ( $n = 3$ ). (c) HEI-OC1 cells were incubated with gentamicin (20  $\mu$ M) for different time intervals under hypoxia condition, and the Bax, Bak, and Bcl-2 expressions were examined by western blot analysis and the quantitative densitometry represented as expressed proteins relative to control group. Results are represented as the mean  $\pm$  s.d. \* $P < 0.05$  compared with vehicle group.

damaged (Figure 3e). Besides synergic toxic effects of ischemia and GM ototoxicity to spiral ganglion neurons, this may be caused by secondary loss to the HC, especially IHC loss.<sup>40</sup> Chronic cochlear changes after aminoglycoside ototoxicity also include degeneration of spiral ganglion neurons.<sup>30</sup> Loss of organ of Corti has been demonstrated to cause a slow but progressive loss of spiral ganglion neurons with variable time courses of different cochlear insults.<sup>30</sup> External insult like noise trauma, aminoglycoside ototoxicity, or cochlear ischemia could induce excessive glutamate release from IHCs into synaptic clefts, which could cause spiral ganglion neuron cell death.<sup>41</sup> In this study, HC loss was not apparent unless animals were treated by a combination of GM and 30-min ischemia; IHC loss was most significant in lower cochlear turns (Figure 2). In upper (apical and third) cochlear turns, mild-to-moderate OHC loss was found, with IHCs relatively unaffected (Figure 2). Also, loss of spiral ganglion neurons appeared in lower cochlear turns in animals receiving combined ischemia/GM treatment (Figure 3e), whereas spiral ganglion neurons remained relatively intact in the upper turns (Figure 3b). To summarize cochlear changes after interaction of ischemia and aminoglycoside: cochlear damage moves from the basal turn toward the apex, occurring first in OHCs and then in IHCs, and afterwards shifting to more central neural structures like spiral ganglion neurons. This differential and orderly pattern of cochlear damage echoes previous study of ototoxicity by prolonged and high dose of aminoglycoside.<sup>42</sup>

Several reasons may explain why ischemia contributes to aminoglycoside ototoxicity. Development of aminoglycoside ototoxicity relates to the diffusion of aminoglycoside into the inner ear and its subsequent binding to cochlear tissues, followed by slow release into inner ear fluid.<sup>9</sup> Entry of

aminoglycoside into cochlear cells includes the attachment of the cationic aminoglycoside molecule to negatively charged cell membrane and entering cochlear cells via endocytosis *in vivo*<sup>43</sup> or by permeating through nonselective cation channels such as mechanosensitive transduction channels at stereocilia tips.<sup>44,27</sup> A regulatable blood-labyrinthine barrier (BLB) for aminoglycoside entry exists at the interface between the perilymphatic and endolymphatic space.<sup>45</sup> Immature or defective BLB has been shown to increase the aminoglycoside ototoxicity such as in newborns.<sup>4</sup> Toxicity of aminoglycoside may therefore relate to the integrity of BLB. GM administered alone would not disrupt endothelial cell junction that constitutes the BLB.<sup>46</sup> Ischemic damage is widely known to alter integrity and permeability of blood-brain barrier,<sup>47</sup> morphologically similar to BLB.<sup>48</sup> Permeability of BLB demonstrably increases when cochlea microcirculatory disorders occur.<sup>49</sup> Oxidative stress such as reactive nitrogen stress, the by-product of ischemia/reperfusion injury, was also shown to disrupt BLB.<sup>50</sup> Using fluorescent GM tracking technique, our study also demonstrated increased uptake of GM after transient cochlear ischemia (Figure 4 and Supplementary Figure 1). Therefore, it is possible that higher GM concentrations may reach the cochlear HCs after transient ischemia and result in the consequent cochlear damage.

Predisposition of aminoglycoside ototoxicity by ischemia/reperfusion injury may also be explained on a cellular level. Currently, aminoglycoside is believed to exert its ototoxicity by increasing a variety of free-radical species, including both ROS and reactive nitrogen species, through an iron-dependent pathway.<sup>2</sup> Formation of free radicals by aminoglycosides is initiated by the iron-aminoglycoside complex that actively reduces molecular oxygen to superoxide by an electron

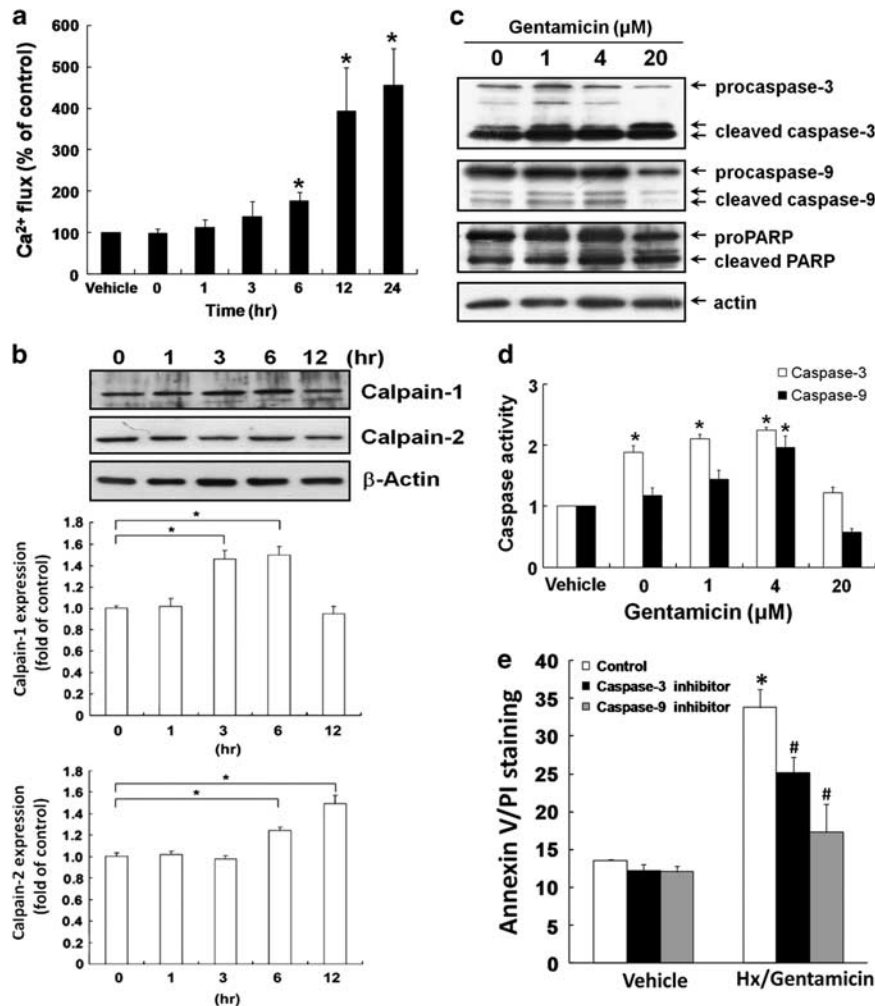


**Figure 9** Ca<sup>2+</sup> release and calpain activity are involved in gentamicin-induced apoptosis of cultured cochlear cells. HEI-OC1 cells were incubated with gentamicin (20 µM) in hypoxia for different time intervals under hypoxia condition. (a) Ca<sup>2+</sup> flux was examined by flow cytometry (n = 3). (b) The protein levels of calpain-1 and calpain-2 were determined by western blot analysis and quantitative densitometry against the control group. (c) Caspase-3 and caspase-9 expressions were examined by western blot analysis. (d) HEI-OC1 cells were incubated with gentamicin (20 µM) for different time intervals under hypoxia condition, and caspase-3 and caspase-9 activities were examined by caspase ELISA kit (n = 3). (e) HEI-OC1 cells were pretreated for 30 min with inhibitors of caspase-3 and caspase-9 followed by stimulation with gentamicin (20 µM) under hypoxia condition for 24 h, and the percentage of apoptotic cells were then analyzed with flow cytometry analysis of Annexin V/PI staining (n = 3). Results are represented as the mean ± s.d. \*P < 0.05 compared with vehicle group; #P < 0.05 compared with control group.

donor and formation of other free radicals ensue.<sup>2,51</sup> Such iron-aminoglycoside complex is believed to mediate free-radical-induced cell damage and initiate apoptotic cascades. Ischemia/reperfusion injury of cochlea has been also shown to elicit release of free iron and massive production of nitric oxide by nitric oxide synthase.<sup>52</sup> Free iron may further chelate with the aminoglycoside, which induces cascades of ROS formation. Such high level of ROS, coupled with the disruption in the BLB, may result in auditory dysfunction or even irreversible hearing loss.

Multiple death pathways, including necrotic and apoptotic pathways, contribute to cochlear HC death after aminoglycoside ototoxicity.<sup>35</sup> In acute administration, apoptosis may be the predominant form of cell death and caspase cascades

were shown to be the downstream pathways.<sup>53</sup> However, both necrotic and apoptotic morphologies were observed in cochlear HCs and caspase-independent apoptosis was shown in chronic aminoglycoside ototoxicity instead of traditional caspase-dependent apoptosis.<sup>35</sup> This study assessed acute interaction of hypoxia and GM, revealing an apoptotic cellular death through a caspase-dependent pathway (Figures 7–9).

The caspase-dependent apoptotic pathway is mediated by activation of caspase through either intrinsic or extrinsic pathways.<sup>54</sup> A previous study shows GM not causing apoptosis through extrinsic apoptotic pathways via Fas receptors,<sup>55</sup> much evidence indicates mitochondrial-dependent intrinsic apoptotic pathways' role in aminoglycoside-induced

cell apoptosis. Genetic and biochemical evidence also portends mitochondrial dysfunction as crucial in susceptibility to aminoglycoside ototoxicity.<sup>56</sup> GM has been proven to elicit release of iron from mitochondria, and to enhance generation of hydroxyl radicals.<sup>57</sup> Our previous study directly demonstrated greater susceptibility to aminoglycoside toxicity from acute mitochondrial dysfunction.<sup>58</sup> In this study, ischemia was interacted with GM *in vitro*, with loss of mitochondrial membrane potential (Figure 8a) observed in the early stage of hypoxia, followed by elevation of oxidative stress (Figure 8b). Caspase cascades are triggered by initiator caspase 9 and executioner caspase 3 (Figure 9c and d), which leads to processing of apoptotic cell death.

In addition to mitochondrial-dependent apoptotic pathway, calcium influx (Figure 9a) and increased expression of calpain (Figure 9b) were observed in the early stage of ischemia interacting with GM *in vitro*. Previous studies have demonstrated that GM may cause a dose-dependent increase in intracellular calcium in chicken HCs.<sup>59</sup> Cellular influx via GM-induced HC damage may activate calpain and precipitate apoptotic cascades.<sup>60</sup>

Interaction between hypoxia/ischemia and aminoglycoside ototoxicity occurs in diverse scenarios: (1) simultaneous application of aminoglycoside and occurrence of hypoxia/ischemia; (2) sub-damaging doses of aminoglycoside enhancing hypoxia/ischemia; and (3) previous hypoxia/ischemia augmenting subsequent aminoglycoside toxicity. The hypoxia/ischemia-then-drug paradigm in this study displayed apparent synergism, implying that ischemia can increase susceptibility to aminoglycoside ototoxicity. This paradigm is more relevant to ordinary clinical situations that the aminoglycoside usually is given when the patient is infected or in hypoperfusion status like sepsis, hypovolemia, or impending shock.

In summary, this study showed direct evidence that ischemia/reperfusion injury may increase the aminoglycoside ototoxicity. This may have crucial implications for clinical practice that it may be vital to remove sources that contribute to cochlear ischemia, such as shock status or hypovolemia. This study can yield further insight relevant to complicated interaction between ischemia and aminoglycoside, plus cytotoxic mechanisms they may induce within cochlea that potentiate ischemia or aminoglycoside ototoxicity into cytotoxic phenomenon. These results should aid the understanding of the interacting mechanism and potential preventive strategy against aminoglycoside ototoxicity.

Supplementary Information accompanies the paper on the Laboratory Investigation website (<http://www.laboratoryinvestigation.org>)

#### ACKNOWLEDGEMENTS

We thank Ms Hui-Chuan Lin for technical assistance in preparation of the specimens. This research was supported in part by Taiwan Department of Health Clinical Trial and Research Center of Excellence (DOH100-TD-B-111-004) and research grants from China Medical University (CMU97-069), China Medical University Hospital (DMR96-121 and DMR99-46).

#### DISCLOSURE/CONFLICT OF INTEREST

The authors declare no conflict of interest.

- Gupta R, Kim JY, Espinal MA, *et al*. Public health. Responding to market failures in tuberculosis control. *Science* 2001;293:1049–1051.
- Forge A, Schacht J. Aminoglycoside antibiotics. *Audiol Neurootol* 2000;5:3–22.
- Contopoulos-Ioannidis DG, Giotis ND, Baliatsa DV, *et al*. Extended-interval aminoglycoside administration for children: a meta-analysis. *Pediatrics* 2004;114:e111–e118.
- Bernard PA. Freedom from ototoxicity in aminoglycoside treated neonates: a mistaken notion. *Laryngoscope* 1981;91:1985–1994.
- Ensink RJ, Camp GV, Cremers CW. Mitochondrial inherited hearing loss. *Clin Otolaryngol Allied Sci* 1998;23:3–8.
- Guan MX, Fischel-Ghodsian N, Attardi G. A biochemical basis for the inherited susceptibility to aminoglycoside ototoxicity. *Hum Mol Genet* 2000;9:1787–1793.
- Fischel-Ghodsian N. Mitochondrial deafness mutations reviewed. *Hum Mutat* 1999;13:261–270.
- Johnson RF, Cohen AP, Guo Y, *et al*. Genetic mutations and aminoglycoside-induced ototoxicity in neonates. *Otolaryngol Head Neck Surg* 2010;142:704–707.
- Tran Ba Huy P, Manuel C, Meulemans A, *et al*. Ethacrynic acid facilitates gentamicin entry into endolymph of the rat. *Hear Res* 1983;11:191–202.
- Bates DE, Beaumont SJ, Baylis BW. Ototoxicity induced by gentamicin and furosemide. *Ann Pharmacother* 2002;36:446–451.
- Guthrie OW. Aminoglycoside induced ototoxicity. *Toxicology* 2008;249:91–96.
- Li H, Steyger PS. Synergistic ototoxicity due to noise exposure and aminoglycoside antibiotics. *Noise Health* 2009;11:26–32.
- Salamy A, Eldredge L, Tooley WH. Neonatal status and hearing loss in high-risk infants. *J Pediatr* 1989;114:847–852.
- Aust G. Vestibulotoxicity and ototoxicity of gentamicin in newborns at risk. *Int Tinnitus J* 2001;7:27–29.
- Chayasirisobhon S, Yu L, Griggs L, *et al*. Recording of brainstem evoked potentials and their association with gentamicin in neonates. *Pediatr Neurol* 1996;14:277–280.
- Axelsson A, Nuttall AL, Miller JM. Observations of cochlear microcirculation using intravital microscopy. *Acta Otolaryngol (Stockh)* 1990;109:263–270.
- Pirodda A, Saggese D, Giausa G, *et al*. Can hypotension episodes cause cochlear damage in young subjects? *Med Hypotheses* 1997;48:195–196.
- Chao TK. Sudden sensorineural hearing loss after rapid reduction of blood pressure in malignant hypertension. *Ann Otol Rhinol Laryngol* 2004;113:73–75.
- Seidman MD, Ahmad N, Bai U. Molecular mechanisms of age-related hearing loss. *Ageing Res Rev* 2002;1:331–343.
- Henderson D, Bielefeld EC, Harris KC, *et al*. The role of oxidative stress in noise-induced hearing loss. *Ear Hear* 2006;27:1–19.
- Thorne PR, Nuttall AL. Laser Doppler measurements of cochlear blood flow during loud sound exposure in the guinea pig. *Hear Res* 1987;27:1–10.
- Wu WJ, Sha SH, McLaren JD, *et al*. Aminoglycoside ototoxicity in adult CBA, C57BL and BALB mice and the Sprague-Dawley rat. *Hear Res* 2001;158:165–178.
- Boettcher FA, Henderson D, Gratton MA, *et al*. Synergistic interactions of noise and other ototraumatic agents. *Ear Hear* 1987;8:192–212.
- Lin CD, Wei IH, Tsai MH, *et al*. Changes in guinea pig cochlea after transient cochlear ischemia. *NeuroReport* 2010;21:968–975.
- Perlman HB, Kimura R, Fernandez C. Experiments on temporary obstruction of the internal auditory artery. *Laryngoscope* 1959;69:591–613.
- Steyger PS, Peters SL, Rehling J, *et al*. Uptake of gentamicin by bullfrog saccular hair cells *in vitro*. *J Assoc Res Otolaryngol* 2003;4:565–578.
- Wang Q, Steyger PS. Trafficking of systemic fluorescent gentamicin into the cochlea and hair cells. *J Assoc Res Otolaryngol* 2009;10:205–219.
- Tang CH, Chiu YC, Huang CF, *et al*. Arsenic induces cell apoptosis in cultured osteoblasts through endoplasmic reticulum stress. *Toxicol Appl Pharmacol* 2009;241:173–181.



29. Jin X, Jin X, Sheng X. Methylcobalamin as antagonist to transient ototoxic action of gentamicin. *Acta Otolaryngol (Stockh)* 2001;121:351–354.
30. Leake PA, Hradek GT. Cochlear pathology of long term neomycin induced deafness in cats. *Hear Res* 1988;33:11–33.
31. Hayashida T, Nomura Y, Iwamori M, *et al*. Distribution of gentamicin by immunofluorescence in the guinea pig inner ear. *Arch Otorhinolaryngol* 1985;242:257–264.
32. Mizukoshi O, Daly JF. Oxygen consumption in normal and kanamycin damaged cochleae. *Acta Otolaryngol* 1967;64:45–54.
33. Thalmann R, Miyoshi T, Thalmann I. The influence of ischemia upon the energy reserves of inner ear tissues. *Laryngoscope* 1972;82:2249–2272.
34. Sha SH, Taylor R, Forge A, *et al*. Differential vulnerability of basal and apical hair cells is based on intrinsic susceptibility to free radicals. *Hear Res* 2001;155:1–8.
35. Jiang H, Sha SH, Forge A, *et al*. Caspase-independent pathways of hair cell death induced by kanamycin in vivo. *Cell Death Differ* 2006;13:20–30.
36. McDowell B. Patterns of cochlear degeneration following gentamicin administration in both old and young guinea pigs. *Br J Audiol* 1982;16:123–129.
37. Suzuki M, Yagi M, Brown JN, *et al*. Effect of transgenic GDNF expression on gentamicin-induced cochlear and vestibular toxicity. *Gene Ther* 2000;7:1046–1054.
38. Tabuchi K, Tsuji S, Fujihira K, *et al*. Outer hair cells functionally and structurally deteriorate during reperfusion. *Hear Res* 2002;173:153–163.
39. Suzuki M, Ushio M, Yamasoba T. Time course of apoptotic cell death in guinea pig cochlea following intratympanic gentamicin application. *Acta Otolaryngol (Stockh)* 2008;128:724–731.
40. Bae WY, Kim LS, Hur DY, *et al*. Secondary apoptosis of spiral ganglion cells induced by aminoglycoside: Fas-Fas ligand signaling pathway. *Laryngoscope* 2008;118:1659–1668.
41. Steinbach S, Lutz J. Glutamate induces apoptosis in cultured spiral ganglion explants. *Biochem Biophys Res Commun* 2007;357:14–19.
42. Kalkandelen S, Selimoglu E, Erdogan F, *et al*. Comparative cochlear toxicities of streptomycin, gentamicin, amikacin and netilmicin in guinea-pigs. *J Int Med Res* 2002;30:406–412.
43. Hashino E, Shero M. Endocytosis of aminoglycoside antibiotics in sensory hair cells. *Brain Res* 1995;704:135–140.
44. Marcotti W, van Netten SM, Kros CJ. The aminoglycoside antibiotic dihydrostreptomycin rapidly enters mouse outer hair cells through the mechano-electrical transducer channels. *J Physiol (Lond)* 2005;567:505–521.
45. Dai CF, Steyger PS. A systemic gentamicin pathway across the stria vascularis. *Hear Res* 2008;235:114–124.
46. Laurell G, Viberg A, Teixeira M, *et al*. Blood-perilymph barrier and ototoxicity: an in vivo study in the rat. *Acta Otolaryngol (Stockh)* 2000;120:796–803.
47. Spatz M. Past and recent BBB studies with particular emphasis on changes in ischemic brain edema. *Acta Neurochir Suppl* 2010;106:21–27.
48. Jahnke K. The blood-perilymph barrier. *Arch Otorhinolaryngol* 1980;228:29–34.
49. Zhang X, Wang J. Effects of microcirculatory disorders of inner ear on blood-labyrinth barrier permeability in guinea pigs. *Chin J Otorhinolaryngol* 2000;35:339–341.
50. Kastenbauer S, Klein M, Koedel U, *et al*. Reactive nitrogen species contribute to blood-labyrinth barrier disruption in suppurative labyrinthitis complicating experimental pneumococcal meningitis in the rat. *Brain Res* 2001;904:208–217.
51. Lesniak W, Pecoraro VL, Schacht J. Ternary complexes of gentamicin with iron and lipid catalyze formation of reactive oxygen species. *Chem Res Toxicol* 2005;18:357–364.
52. Tabuchi K, Tsuji S, Asaka Y, *et al*. Ischemia-reperfusion injury of the cochlea: effects of an iron chelator and nitric oxide synthase inhibitors. *Hear Res* 2001;160:31–36.
53. Ylikoski J, Xing-Qun L, Virkkala J, *et al*. Blockade of c-Jun N-terminal kinase pathway attenuates gentamicin-induced cochlear and vestibular hair cell death. *Hear Res* 2002;166:33–43.
54. Rybak LP, Kelly T. Ototoxicity: bioprotective mechanisms. *Curr Opin Otolaryngol HN Surg* 2003;11:328–333.
55. Bodmer D, Brors D, Pak K, *et al*. Gentamicin-induced hair cell death is not dependent on the apoptosis receptor Fas. *Laryngoscope* 2003;113:452–455.
56. Guan MX. Molecular pathogenetic mechanism of maternally inherited deafness. *Ann NY Acad Sci* 2004;1011:259–271.
57. Walker PD, Barri Y, Shah SV. Oxidant mechanisms in gentamicin nephrotoxicity. *Ren Fail* 1999;21:433–442.
58. Lin CD, Oshima T, Oda K, *et al*. Ototoxic interaction of kanamycin and 3-nitropropionic acid. *Acta Otolaryngol (Stockh)* 2008;128:1280–1285.
59. Hirose K, Westrum LE, Stone JS, *et al*. Dynamic studies of ototoxicity in mature avian auditory epithelium. *Ann NY Acad Sci* 1999;884:389–409.
60. Ding D, Stracher A, Salvi RJ. Leupeptin protects cochlear and vestibular hair cells from gentamicin ototoxicity. *Hear Res* 2002;164:115–126.